Journal of Solid State Chemistry 190 (2012) 226–232

Contents lists available at SciVerse ScienceDirect

Journal of Solid State Chemistry

journal homepage: www.elsevier.com/locate/jssc

Synthesis, crystal growth, structural and physicochemical studies of novel binary organic complex: 4-chloroaniline–3-hydroxy-4-methoxybenzaldehyde

K.P. Sharma, R.S.B. Reddi, S. Bhattacharya, R.N. Rai *

Department of Chemistry, Centre of Advance Study, Banaras Hindu University, Varanasi-221005, India

ARTICLE INFO

Article history:
Received 6 June 2011
Received in revised form
26 January 2012
Accepted 5 February 2012
Available online 17 February 2012

Keywords:
Phase equilibria
Crystal growth
Optical properties
Crystal packing: X-ray diffraction
Band gap

ABSTRACT

The solid-state reaction, which is solvent free and green synthesis, has been adopted to explore the novel compound. The phase diagram of 4-chloroaniline (CA) and 3-hydroxy-4-methoxybenzaldehyde (HMB) system shows the formation of a novel 1:1 molecular complex, and two eutectics on either sides of complex. Thermochemical studies of complex and eutectics have been carried out for various properties such as heat of fusion, entropy of fusion, Jackson's parameters, interfacial energy and excess thermodynamic functions. The formation of molecular complex was also studied by IR, NMR, elemental analysis and UV–Vis absorption spectra. The single crystal of molecular complex was grown and its XRD study confirms the formation of complex and identifies the crystal structure and atomic packing of crystal of complex. Transmission spectra of grown crystal of the complex show 70% transmittance efficiency with cut off wavelength 412 nm. The band gap and refractive index of the crystal of complex have also been studied.

1. Introduction

The metallic systems are potential candidates for technological applications as well as for fundamental studies till the revolution of organic materials. The limited choices of materials, density driver convection effect, opacity, high transformation temperature, difficulties involved in experimentation and cost factors, are the limiting factors to work with the metallic systems [1,2]. To cater the needs of current civilization, synthesis and characterization of novel materials with special features and of low cost are demanding. Organic materials are known for their various promising properties [3,4] and the pure as well as binary organic materials have been found worthwhile for nonlinear optical, fluorescent and white light emitting materials [5–8]. Further, organic systems, their eutectics and addition compounds/complexes are the analogs of metallic systems [9], and initially the organic systems were considered as model systems to study the mysteries of various fundamental aspects which affect the properties of materials. However, the synthesis of novel materials utilizing solid state reaction has additional merits such as 100% yield of materials and solvent free synthesis. The synthesis of complex of 2-methoxy-5-[[(4-chlorophenyl)imino] methyl] phenol (Registry No. 115095-36-8) is reported by other method [10]. However there is no report for synthesis of this complex adopting solid state reaction, phase diagram, and various other studies which are being mentioned in this article. With view to explore the concept of phase diagram and solid state reaction, a binary organic system involving 4-chloroaniline (CA) and 3-hydroxy-4-methoxybenzaldehyde (HMB) was selected. The solid state reaction was employed [11] to establish the phase diagram and to synthesis of binary materials. In this communication the phase diagram study, and the synthesis and physicochemical studies of addition compound and two eutectics, along with crystallization behavior of pure and binary materials, are reported. The interaction between CA-HMB molecules, single crystal growth, atomic packing, optical characterization, band gap and refractive index of the newly synthesized addition compound are also reported. However, the other characterizations of crystalline and polycrystalline binary addition compound are in progress.

2. Experimental procedure

2.1. Materials and purification

Starting materials, 4-Chloroaniline and 3-hydroxy-4-methoxybenzaldehyde were obtained from Sigma Aldrich, Germany. Both the materials were purified by recrystallization from ethanol. The melting temperatures of purified CA and HMB were found to be

* Corresponding author. Fax: +91 542 2307321.
E-mail address: rn_rai@yahoo.co.in (R.N. Rai).

0022-4596/$ - see front matter © 2012 Elsevier Inc. All rights reserved.
doi:10.1016/j.jssc.2012.02.019

69.0 and 113.0 °C, respectively. The values of melting temperature are in agreement with their respective literature values [6,7].

2.2. Phase diagram

The phase diagram of CA–HMB system was established in the form of melting temperature–composition curve [12]. The mixtures of two components covering the entire range of compositions were taken in separate test tubes. The mouth of each test tube was sealed and the melt of mixtures of two components were homogenized by repeating the process of melting followed by chilling in ice cooled water for 4 times. The melting points of the various compositions, thus synthesized, were determined using Toshniwal melting point apparatus attached with a precision thermometer of accuracy ± 0.5 °C.

2.3. Enthalpy of fusion

The values of heat of fusion of the pure components, the eutectics and the complex were determined by differential scanning calorimeter (Mettler DSC-4000 system). Indium sample was used to calibrate the system and the amount of test sample and heating rate were about 5–7 mg and 10 °C min^{-1}, respectively. The values of enthalpy of fusion are reproducible within ± 0.01 kJ mol^{-1}.

2.4. Growth kinetics

The solidification behavior of pure components, eutectics and addition compound were determined by measuring the rate of movement of solid liquid interface in a thin glass U-tube with about 150 mm horizontal portion and 5 mm internal diameter. Molten samples were separately taken in U-tube and placed in a silicone oil bath. The temperature of oil bath was maintained using microprocessor temperature controller of accuracy ± 0.1 °C. At different undercoolings (ΔT), a seed crystal of the same composition was added to start nucleation, and the rate of movement of the solid–liquid interface (v) was measured using a traveling microscope and a stop watch [12].

2.5. Spectral studies

Infrared spectra of the parent components and the complex were recorded in the spectral region 400–4000 cm^{-1} via pelletizing the materials that was dispersed in KBr using Perkin–Elmer RX-1, FT-IR spectrophotometer. The ^{1}H and ^{13}C NMR spectra were measured in JEOL 300 FTNMR using $CDCl_3$ as a solvent. The data of elemental analysis for complex compound was recorded using the CHN/Elemental Analyzer (Exeter Analytical, Inc. Model 440, USA).

2.6. Single crystal growth and study of atomic packing

The single crystal of the novel complex was grown from the saturated ethanol solution at room temperature by slow evaporation technique. X-ray diffraction data of single crystal were collected using the Xcalibur oxford CCD diffractometer. The data reduction was carried out using Chrysalis Pro software. Structure solution and refinement were carried out utilizing SHELXS and SHLEXL-97 [13].

2.7. Optical characterization

The optical transmittance of the grown crystal was recorded in UV–Vis–NIR spectrophotometer [JASCO V-670, Tokyo, Japan] in the range of 190–950 nm. For comparison, the absorbance spectra of parent components and its complex were also recorded in ethanol solution using the same instrument.

3. Results and discussions

3.1. Phase diagram

The phase diagram of the CA-HMB system, established in terms of composition and their respective melting temperatures, is given in Fig. 1. The melting point of HMB (113.0 °C) decreases with the addition of CA and attains the minimum temperature (99.0 °C) at 0.225 mol fraction of CA. This point is known as the first eutectic point (E_1) of the system. Further addition of CA in HMB the melting point rises and reaches to a maximum melting temperature (138.5 °C) at point *C*, where the composition of CA and HMB are 1:1 *M* ratio. This composition forming the molecular complex or addition compound melts congruently, i.e., liquid has identical composition of the solid. When mole fraction of CA increases beyond this composition, the melting point again decreases till the second eutectic (E_2). The melting temperature and mole fraction of CA at E_2 are 64.0 °C and 0.920, respectively. The addition of CA thereafter causes an increase in the melting point till 69.0 °C, which is the melting point of CA. The finding of maximum melting temperature, even more than parent components, of complex and flat nature of curve suggests the formation of a stable new entity [14]. This observation also infers that the complex does not dissociate in molten state. For each eutectic, the molecular complex behaves as one of the parent component. The phase diagram study reveals that there are three invariant points, eutectic-1, complex and eutectic-2, in the HMB-CA system.

3.2. Growth kinetics

In order to study the crystallization behaviors of the pure components, eutectics, and the complex, the crystallization rate (v) are determined at different undercoolings (ΔT) by measuring the rate of movement of solid-liquid interface in a thin glass U-tube. The plots between log ΔT and log v for pure compounds and binary materials are given in Fig. 2. The graph, for each material, shows the linear dependence which is in accordance with following equation

$$v = u(\Delta T)^n \quad (1)$$

where u and n are constants depending on the solidification behavior of the materials. The experimental values of these constants for pure components, eutectics and addition compound are given in Table 1. From the values of u, it can be inferred that the growth velocity of eutectic E_1 is less than those of its components namely HMB and addition compound while that of E_2 lies in between CA and addition compound. In case of E_1, the melting point of addition compound is higher than that of HMB and hence addition compound nucleates first followed by the nucleation of HMB and the two phases grow by the alternate nucleation mechanism. On the other hand in E_2 the addition compound, with higher melting point than CA, nucleates first followed by nucleation of CA and the two phases grow following the side by side mechanism [15].

3.3. Thermochemistry

3.3.1. Enthalpy of fusion

The experimental values of enthalpy of fusion of the pure components, the eutectics and the addition compound are given in Table 2. For the purpose of comparison the heats of fusion of eutectics are calculated by the mixture law [9] and have tabulated

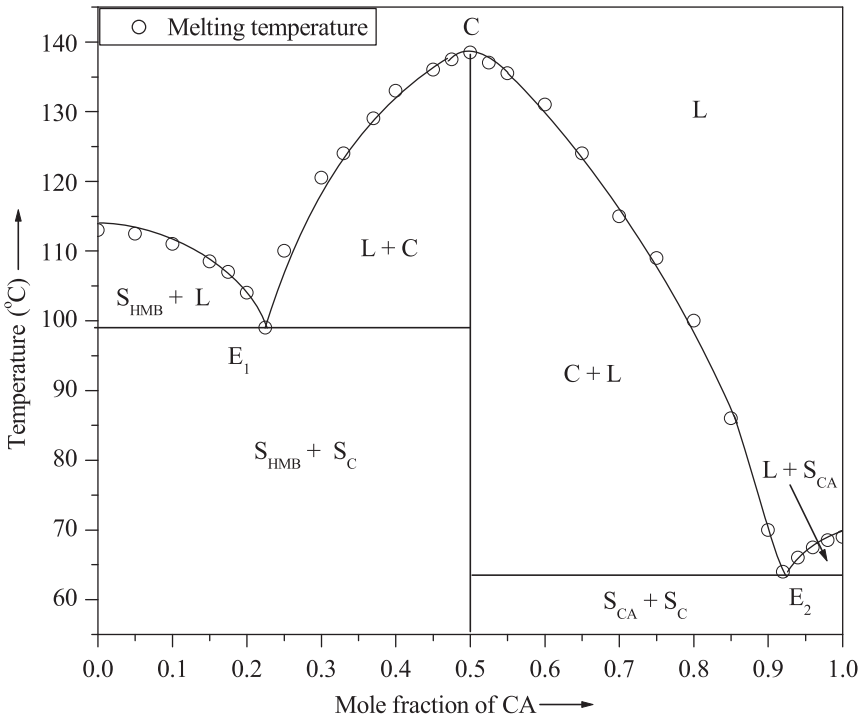

Fig. 1. Phase diagram of 4-chloroaniline–3-hydroxy-4-methoxybenzaldehyde system.

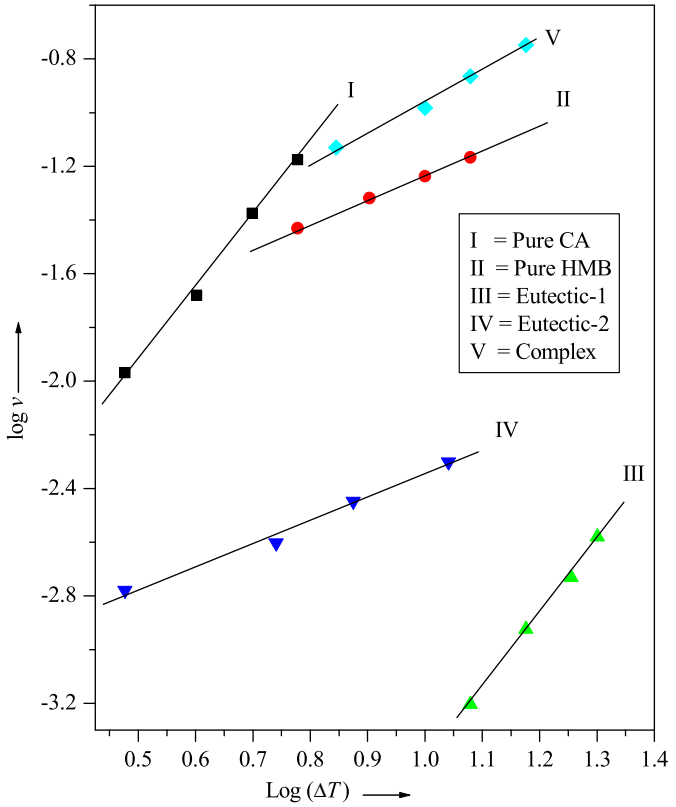

Fig. 2. Linear velocity of crystallization at various degrees of undercooling for pure components, eutectics and complex.

in the same table. The values of enthalpy of mixing which is the difference of experimental and the calculated values of the enthalpy of fusion of the eutectic-1 and eutectic-2 are found to be -5.1 and -1.7 kJ mol^{-1}. As such, three types of structures are

Table 1
Values of n and u for pure components and their eutectics, and complex.

Material	n	u (mm s^{-1} deg^{-1})
CA	2.67	5.51×10^{-4}
HMB	0.87	7.76×10^{-3}
Eutectic-1	2.76	6.54×10^{-7}
Eutectic-2	0.85	6.29×10^{-4}
Complex	1.16	7.53×10^{-3}

suggested [16]; quasi-eutectic for $\Delta_{mix}H > 0$, clustering of molecules for $\Delta_{mix}H < 0$ and molecular solution for $\Delta_{mix}H = 0$. The highly negative value of enthalpy of mixing in both eutectics suggests that there is associative interaction in the molecules in the eutectic melt. The entropy of fusion ($\Delta_{fus}S$) values, for different materials, has been calculated by dividing the enthalpy of fusion by their corresponding absolute melting temperatures (Table 2). The positive values suggest that the entropy factor favors the melting process.

3.3.2. *Interfacial energy and size of critical radius*

During crystallization process, when liquid is cooled below its melting temperature it does not solidify spontaneously because under equilibrium condition the melt contains number of clusters of molecules. As long as the clusters are well below the critical size, they can not grow to form crystals. The critical size (r^*) of nucleus is related to interfacial energy (σ) by [17].

$$r^* = \frac{2\sigma T_{fus}}{\Delta_{fus}H \cdot \Delta T} \tag{2}$$

where T_{fus}, $\Delta_{fus}H$ and ΔT are melting temperature, heat of fusion, and degree of undercooling, respectively. However, the interfacial energy is computed by using the expression [17]

$$\sigma = \frac{C \cdot \Delta_{fus}h}{(N_A)^{1/3}(V_m)^{2/3}} \tag{3}$$

Table 2
Melting point, heat of fusion, entropy of fusion and interfacial energy of pure. components and their eutectics, and complex.

Materials	Melting temperature (K)	Heat of fusion (kJ mol^{-1})	Heat of mixing (kJ mol^{-1})	Entropy of fusion (J mol^{-1} K^{-1})	Interfacial energy (kJ m^{-2}) $\times 10^{-6}$
CA	342.0	22.38		65.44	46.43
HMB	386.0	29.55		76.55	48.42
Eutectictic-1					
(Exp.)	372.0	22.84	−5.10	61.40	47.98
(Cal.)		27.90			
Eutectictic-2					
(Exp.)	337.0	21.18	−1.70	62.85	46.57
(Cal.)		22.88			
Complex	411.5	23.28		56.57	47.43

Table 3
Critical radius of pure components and their eutectics, and complex.

Undercooling ΔT °C)	Critical radius $\times 10^{-8}$ cm				
	CA	HMB	Eutectic-1	Eutectic-2	Complex
3.0	4.37			4.94	
3.5				4.23	
4.0	3.55				
5.0	2.84				
5.5				2.69	
6.0	2.37	2.11			
7.0					2.40
7.5				1.98	
8.0		1.58			
10.0		1.26			1.68
11.0				1.35	
12.0		1.05	1.30		1.40
15.0			1.04		1.12
18.0			0.87		
20.0			0.78		

Table 4
Excess thermodynamic functions for eutectics.

Material	g^E (kJ mol^{-1})	h^E (kJ mol^{-1})	s^E (kJ mol^{-1} K^{-1})
Eutectic-1	−0.1138	25.157	0.0679
Eutectic-2	0.0661	−14.628	−0.0436

where N_A is the Avogadro number, V_m is the molar volume, and the values of parameter C lies between 0.34 and 0.45. The interfacial energy and critical nucleus at different undercoolings, for different materials, are reported in Tables 2 and 3, respectively. It is evident from the table that the radius of critical nucleus decreases with increasing undercooling.

3.3.3. Excess thermodynamic functions

The deviation from the ideal behavior can best be expressed in terms of excess thermodynamic functions, namely, excess free energy (g^E), excess enthalpy (h^E), and excess entropy (s^E) which give a more quantitative idea about the nature of molecular interactions. The excess thermodynamic functions can be calculated by using earlier reported equations [16, 18], and the calculated various excess thermodynamic functions are given in Table 4.The negative value of excess free energy; g^E for E_1 suggests that the interactions between unlike molecules are stronger than those between like molecules while the positive value for E_2 infers the strong interaction between like molecules [17]. The values of h^E and s^E, complementary to g^E, are the measure of excess enthalpy and excess entropy of mixing, respectively.

3.4. Spectral studies

To understand the nature of interaction between HMB and CA molecules, the infrared and NMR studied have been done and the significant changes due to the bond formation have been considered. The FT-IR spectrum of CA gives two sharp peaks at 3380 cm^{-1} and 3470 cm^{-1} due to symmetric and antisymmetric N–H stretching and another sharp peak at 1614 cm^{-1} due to N–H deformation of –NH_2 group while a sharp peak at 1672.7 cm^{-1} was assigned for C=O group in FT-IR spectrum of HMB. In the FT-IR spectrum of complex formed; the peaks for –NH_2 and C=O groups were disappeared and a new peak at 1582.5 cm^{-1} was appeared which corresponds to the C=N stretching.

The proton NMR spectra of HMB shows a signal at δ 9.87 due to the carbonyl proton (–CHO) and CA gives a peak at δ 4.0 due to –NH_2 protons. In the NMR spectra of complex both peaks disappear and a new signal at δ 8.37 was recorded which could be due to the –N=CH– proton.

In ^{13}C NMR spectra, HMB shows a peak at δ 190 due to carbonyl (–CHO) carbon and CA shows a signal at δ 144.8 corresponding to C–NH_2 carbon. In the addition compound both signals disappear and a new peak at δ 161.9 appears which also corresponds to the –N=CH– carbon. From the spectral studies it could be concluded that –NH_2 group of CA and –CHO group of HMB are involved in the bond formation and give strong indicative for the formation of new complex.

The elemental analysis gives the quantitative information about % composition of the elements (C, H and N) present in the compound. The experimental elemental analysis of the complex compound for C, H and N are found to be 64.206, 4.410 and 4.987%, respectively, and these values are very close to their respective computed values (64.249, 4.622 and 5.352%).

3.5. Single crystal growth and crystal X-ray diffraction

The single crystal of newly synthesized complex was grown from saturated solution of ethanol using slow evaporation technique at 303 K. The transparent crystal of the size $22 \times 4 \times 2$ mm^3 was grown in 30 day (Fig. 3). In literature, the crystal structures of HMB was found monoclinic with space group $P2_1/a$ and lattice constants a=8.51 Å, b=13.42 Å, c=6.43 Å [19], and CA has reported for orthorhombic crystal structure with $Pn2_1a$ space group and lattice constants a=8.665 Å, b=7.397 Å and c=9.281 Å [20]. However, the single crystal X-ray diffraction analysis of complex infers that it has crystallized in monoclinic unit cell with $P2_1/n$ space group. The lattice parameters as well as various other crystallographic parameters of the crystal are given in Table 5, and selected bond angle and bond length between different atoms of complex molecule have given in Table 6. The picture of experimental powder X-ray diffraction (PXRD) pattern of complex compound has been given in Supplementary Fig. S-I. The molecular

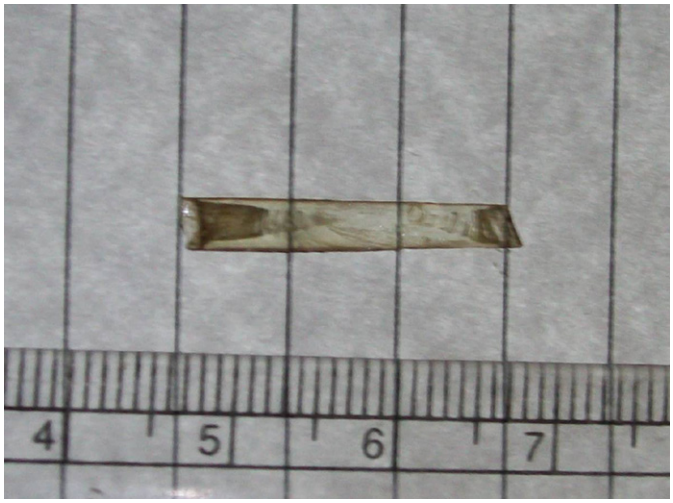

Fig. 3. Photograph of the grown crystal of complex.

Table 5
Crystal data and structure refinement table for complex crystal.

Empirical formula	$C_{14}H_{12}ClNO_2$
Mw	261.70
T (K)	293
Crystal system	Monoclinic
Space group	$P2_1/n$
a (Å)	15.0582(7)
b (Å)	5.3092(2)
c (Å)	15.8846(7)
β (deg.)	99.396(4)
V (Å^3)	1255.13(9)
Z	4
Exptl. crystal density	1.385 mg/mm^3
μ (Mo K_α/mm^{-1})	0.297
Final *R* indices	$R_1=0.046$
I (*I* > 2s (I))	$wR_2=0.1164$
R indices all data	$R_1=0.075$
	$R_2=0.1279$
GOF on F^2	0.927 Å

Table 6
Selected bond lengths and bond angles for complex crystal.

Bond	Length (Å)
Cl1–C01	1.745 (2)
O02–C11	1.354 (2)
O02–C14	1.434 (2)
O01–C10	1.354 (2)
N01–C07	1.274 (2)
N01–C04	1.418 (2)
C08–C07	1.453 (2)
Bond	**Angle (deg.)**
C11–O02–C14	117.0 (1)
C07–N01–C04	119.2 (2)
O02–C11–C10	115.4 (1)
O02–C11–C12	125.5 (2)
N01–C07–C08	125.5 (2)
O01–C10–C11	116.0 (1)
O01–C10–C09	124.0 (2)
Cl1–C01–C02	119.5 (2)
Cl1–C01–C06	120.1 (2)

structure and numbering scheme of complex are shown in (Fig. 4). The complex molecules are bonded with each other via intermolecular hydrogen bonding. The hydrogen bond exists between H-atom

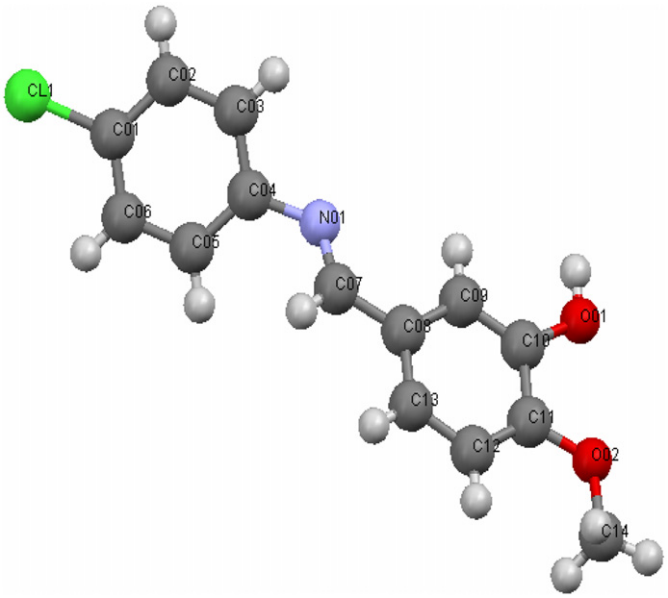

Fig. 4. The molecular structure and numbering scheme of complex.

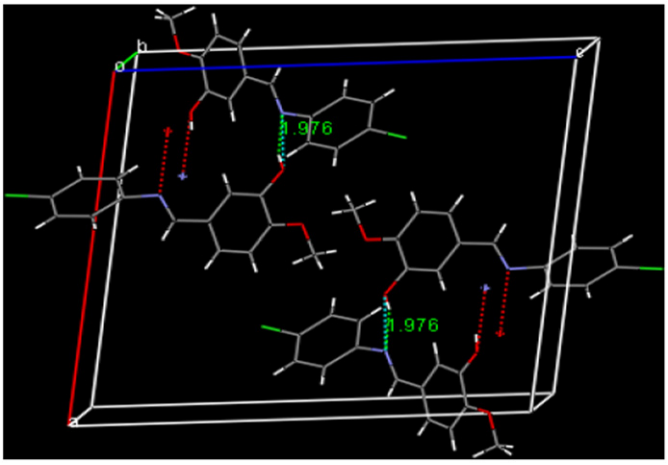

Fig. 5. Crystal packing and hydrogen bonding in the grown crystal of complex.

of OH group of a complex molecule and the N-atom of another neighboring complex molecule (Fig. 5). Each N⁻H bond length is found to be 1.976 Å. Besides this interaction, another interaction between hydrogen atoms and π-electron cloud, i.e., intermolecular C–H⁻π interaction was also observed. The centeroide to H distance is found to be 4.07 Å, (Fig. 6). The two phenyl rings of the complex molecule are non-planar and the interplanar angle was found to be 40.12°.

3.6. Optical characterization

The optical transmittance spectrum of 2 mm thick and hand polished single crystal of complex was determined in the region 190 to 850 nm and has shown in Fig. 7. The transmittance of the crystal was found to be 70% and it was transparent from 412 to 850 nm. Below 412 nm wavelength, the crystal was opaque. For comparative study of the nature of complex, the absorption technique was also extended for pure components and complex in ethanol solution. The absorption peaks of complex compound were significantly different from the absorption peaks of parent components (Fig. 8) which further supports the formation of complex.

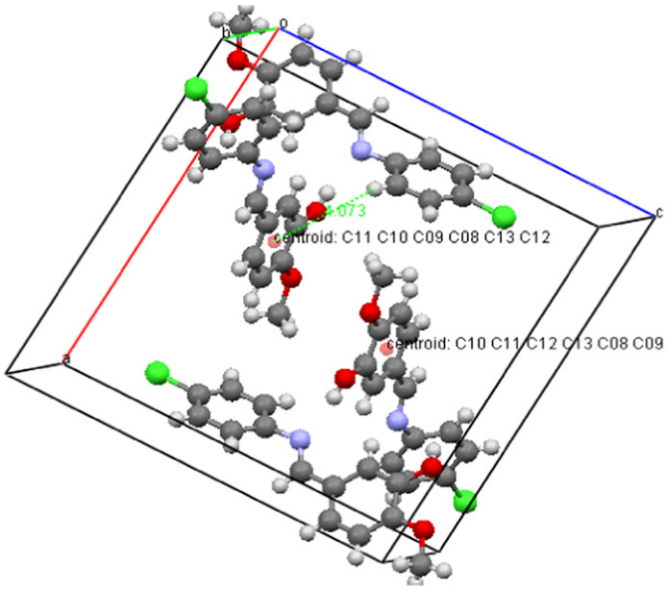

Fig. 6. C–H…π interaction in complex molecules.

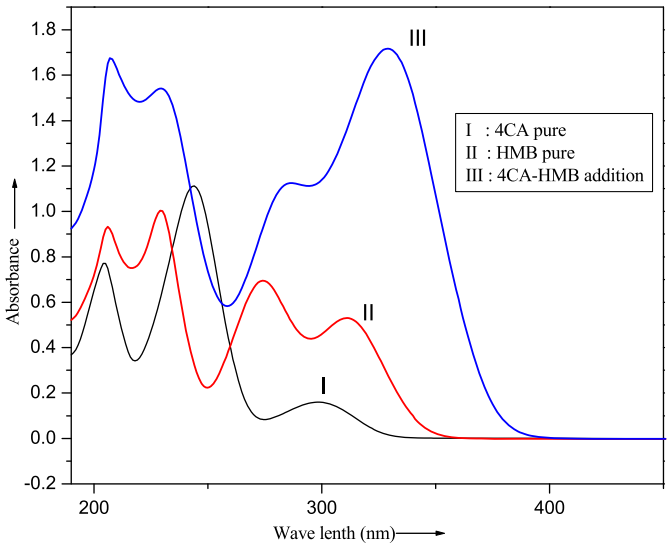

Fig. 8. Absorption spectra of parent compounds and complex.

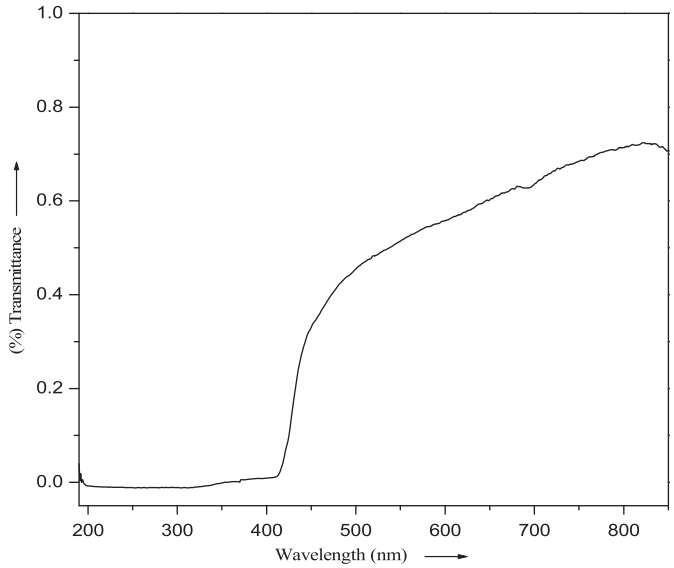

Fig. 7. Transmittance spectra of the grown crystal of complex.

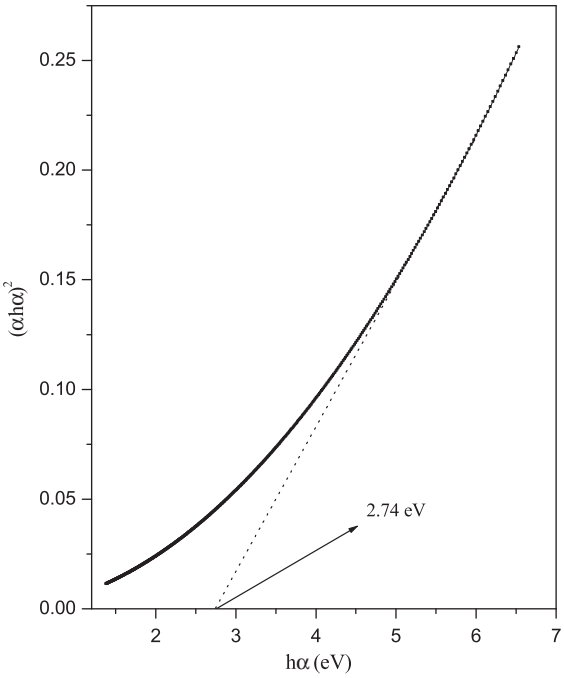

Fig. 9. Plot of α versus photon energy for complex crystal.

3.6.1. *Energy band gap and refractive index*

The optical absorption coefficient, α, for complex crystal at different wavelength was calculated by using the following relation,

$$\alpha = \frac{1}{d}\log(1/T) \tag{4}$$

where T is the transmittance and d the thickness of the crystal. As an indirect band gap material, the crystal has an absorption coefficient (α) obeying the following relation for high photon energies ($h\nu$)

$$\alpha = A\frac{(h\nu - E_g)^2}{h\nu} \tag{5}$$

where E_g is the optical band gap of the crystal and A is a constant. The variation of $(\alpha h\nu)^2$ versus $(h\nu)$, for complex crystals is shown in Fig. 9, and E_g was evaluated [21] from an extrapolation of the linear portion of the curve and it was found to be 2.74 eV. The refractive index of complex crystal was calculated using the relation

$$\frac{n^2-1}{n^2+2} = 1-\sqrt{E_g/20} \tag{6}$$

proposed by Dimitrov and Sakka [22]. The calculated refractive index of complex crystal was found to be 2.45.

4. Conclusions

The binary phase diagram of 4-chloroaniline and 3-hydroxy-4-methoxybenzaldehyde shows the formation of an addition/complex compound and two eutectics on either sides of complex. The

newly synthesized complex and eutectics have been studied for their various thermochemical properties such as heat of fusion, entropy of fusion, interfacial energy and excess thermodynamic functions. The spectral studies, FT-IR, proton and ^{13}C NMR, conclude that parent compounds are covalently bonded, where $-NH_2$ group of CA and –CHO group of HMB are involved in the bond formation, to produce the complex molecule. The experimental elemental analysis of the complex compound for C, H and N is in agreement with the calculated values. The single crystal grown from the saturated solution indicates that the optical quality crystal of complex could be grown. The X-ray diffraction of crystal infers that the complex has crystallized in monoclinic unit cell with $P2_1/n$ space group. The XRD confirms the covalent bonding between parent components to engineer the complex compound. Apart from the covalent bonding there is H- bonding between complex molecules and intermolecular C—H$^-\pi$ interaction. The grown single crystal of the complex was transparent from 412 to 850 nm with 70% transmittance efficiency. The energy band gap and the refractive index of the complex crystal were determined to be 2.74 eV and 2.45, respectively.

Acknowledgments

The authors sincere thank to Board of Research in Nuclear Science, Department of Atomic Energy, Mumbai, India for financial support.

Appendix A. Supplementary materials

Supplementary data associated with this article can be found in the online version at doi:10.1016/j.jssc.2012.02.019.

References

[1] B. Majumdar, K. Chattopadhyay, Met. Trans. A 27 (A) (1996) 2053–2057.
[2] R.N. Rai, J. Mater. Res. 19 (2004) 1348–1355.
[3] W.F. Kaukler, D.O. Frazier, Nature 323 (1986) 50–52.
[4] R.N. Rai, C.W. Lan, J. Mater. Res. 17 (2002) 1587–1591.
[5] P. Gunter, Nonlinear Optical Effects and Materials, Springer-Verlag, Berlin, 2000, p. 540.
[6] A. Yasuhara, A. Kasano, T. Sakamoto, J. Org. Chem. 64 (1999) 2301–2303.
[7] A.K. Mitra, N. Karchaudhuri, A. De, J. Chem. Res. 3 (2004) 237–239.
[8] Y. Dwivedi, S. Kant, R.N. Rai, S.B. Rai, Appl. Phys. B 101 (2010) 639–642.
[9] U.S. Rai, R.N. Rai, J. Cryst. Growth 191 (1998) 234–242.
[10] E. Gunic, I. Tabakovic, J. Org. Chem. 53 (1988) 5081–5087.
[11] G. Rothenberg, A.P. Downie, C.L. Raston, J.L. Scott, J. Am. Chem. Soc. 123 (2001) 8701–8708.
[12] K.P. Sharma, R.S.B. Reddi, S. Kant, R.N. Rai, Thermochim. Acta 498 (2010) 112–116.
[13] G.M. Sheldirck, Shelex-97, Program for Crystal Structure Refinement from Diffraction Data, University of Gottingen, Gottingen, 1997.
[14] U.S. Rai, R.N. Rai, Mol. Mater. 9 (1998) 235–250.
[15] U.S. Rai, R.N. Rai, J. Mater. Res. 14 (1999) 1299–1305.
[16] R.N. Rai, U.S. Rai, Thermochim. Acta 363 (2000) 23–28.
[17] U.S. Rai, R.N. Rai, J. Therm. Anal. 53 (1998) 883–893.
[18] K.P. Sharma, R.N. Rai, J. Mater. Sci. 46 (2011) 1551–1556.
[19] H.A. Rose, Anal. Chem. 28 (1956) 267–268.
[20] J.H. Palm, Acta Crystallogr. 21 (1966) 473–476.
[21] A.K. Chawla, D. Kaur, R. Chandra, Opt. Mater. 29 (2007) 995–998.
[22] V. Dimitrov, S. Sakka, J. Appl. Phys. 79 (1996) 1736–1740.